Am J Transl Res 2019;11(3):1255-1269
www.ajtr.org /ISSN:1943-8141/AJTR0090830

Original Article

Herceptin-conjugated liposomes co-loaded with doxorubicin and simvastatin in targeted prostate cancer therapy

Ning Li[1,2*], Xi Xie[1*], Yixuan Hu[1,2], Huadong He[1], Xian Fu[1], Tiantian Fang[1,3], Changjiu Li[1,2]

[1]Department of Urology, Affiliated Hangzhou First People's Hospital, School of Medicine, Zhejiang University, Hangzhou 310006, China; [2]Nanjing Medical University, Nanjing 211166, China; [3]Zhejiang Chinese Medical University, Hangzhou 310053, China. [*]Equal contributors.

Received December 18, 2018; Accepted January 4, 2019; Epub March 15, 2019; Published March 30, 2019

Abstract: Prostate cancer (PCa) is a leading cause of cancer-related deaths among men. The anthracycline doxorubicin (DOX) is used for the treatment of this disease, but its considerable side effects and non-selectivity are major drawbacks. Simvastatin (Sim), a lipid-lowering agent, holds great promise as a cancer therapeutic, and thus could be used in combination with DOX. Targeted drug-loaded nano-carriers with antibodies for receptors that are overexpressed on tumor cells are promising strategies for decreasing toxicity to normal tissues and enhancing the efficacy of chemotherapies in cancer treatment. Specifically, human epidermal growth factor 2 is overexpressed and constitutively activated in the PC-3 cell line. Within this context, we designed a co-delivery system coated with Herceptin for PCa, performed physicochemical characterizations, and tested the formulations for cytotoxicity and uptake. The targeted liposomes had a mean particle size of 134 nm, and the drug encapsulation efficiency of both Sim and DOX were greater than 80%. We discovered that the drug combination led to the strong inhibition of PCa both *in vitro* and *in vivo,* with inhibitory rates of tumor volumes corresponding to 80.36% and 68.77% of Herceptin-coated liposomes and non-targeted liposomes, respectively. We also found that the anti-tumor mechanisms of the DOX and Sim combination were possibly attributed to synergistic anti-angiogenesis. These results reveal that Herceptin-conjugated liposomes co-loaded with DOX and Sim are a potential novel therapeutic strategy for overcoming PCa.

Keywords: Prostate cancer, HER-2, doxorubicin, simvastatin, liposome

Introduction

Prostate cancer (PCa) is a complex and multifactorial disease, and its occurrence increases rapidly with age [1, 2]. It is the second most recurrently diagnosed cancer and a leading cause of cancer-related deaths among males worldwide [3]. PCa can be treated by various therapies, such as radiotherapy and/or prostatectomy, which have led to major advances in the control of localized and early-stage disease [4-6]. In addition, androgen suppression is a well-established treatment for metastatic PCa [7]. However, patients not cured by these therapies will ultimately develop resistance, resulting in the development of castration-resistant and highly aggressive PCa [8]. Castration-resistant PCa usually has a poor prognosis with a median survival of 9-30 months [9]. For castration-resistant and metastatic PCa, the effectiveness of normal therapies is limited.

In such a situation, chemotherapeutics, one of the most important cancer treatments, generally includes docetaxel, enzalutamide, abiraterone, and sipuleucel [10]. Nonetheless, these survival-enhancing drugs only slightly extend the life span, as they are often restricted by serious adverse effects or lack of efficacy. Moreover, PCa is moderately resistant to cytotoxic therapy, possibly by limiting the drug concentration in cancer cells. Accordingly, novel drugs and drug delivery systems are necessary for patients with advanced castration-resistant PCa [11].

Recent studies have shown that Simvastatin (Sim), a lipid-lowering agent, can affect cancer cell survival and inhibit the growth of multiple

solid tumors, such as breast, colon, lung, ovarian, and prostate cancers, as well as blood cancer, including leukemia [12, 13]. In line with these retrospective studies, Sim was shown to have good potential as a PCa therapeutic [14]. However, the mechanisms of its anticancer effect remain unclear. Some previous studies have reported that statins arrest the cell cycle, induce apoptosis, inhibit tumor metastasis [15, 16], and decrease intracellular cholesterol levels in androgen-independent PCa cells [17]. In this study, we determined whether the new combination therapy of statins and DOX altered the expression of vascular endothelial growth factor (VEGF) and cluster of differentiation 31 (CD-31) in the PC-3 PCa cell line. The key obstacle to achieving the ideal therapeutic effects of conventional chemotherapy is the lack of targeted drug delivery to cancers, as drugs cannot be effective until they are delivered to the target site. In this context, nanotechnology, (e.g., nanoparticles and liposomes) has emerged as a novel approach for delivering drugs to selected cells [18]. Although nanoparticles have the potential to improve the diagnosis and therapeutic efficacy of anticancer agents [19], after surveying the literature from the past 10 years, a survey review showed that only 0.7% (median data) of the nanoparticle dose was delivered to the targeted solid tumors [20]. This drawback may contribute to the low enhanced permeation and retention effects in human tumors, and passive targeting cannot achieve ideal effects. However, these hurdles could be circumvented through surface modification with ligands that target the cancer cells by active targeting [21]. Among the different kinds of targeting ligands, antibodies are one of the most efficacious moieties for specificity and variability.

A prior investigation reported higher expression levels of the human epidermal growth factor receptor-2 (HER-2) in some cancers, including PCa, which were significantly less expressed in normal tissue [22]. Herceptin, a recombinant humanized monoclonal antibody, can target cellular drug delivery as a homing ligand by binding to the HER-2 receptor [23], thereby serving as an important target for antibody-drug-conjugated therapy [24], as well as immunoliposomes [25] and chemo-photothermal therapy [26].

In this study, a Herceptin-liposome for achieving the co-delivery of DOX and Sim was constructed. Then the subsequent specific cellular targeting of this nanosystem and the possible therapeutic effects *in vitro* and *in vivo* were investigated using a HER-2-expressing human PCa cell line (PC-3) as a model (**Scheme 1**).

Materials and methods

Materials

Doxorubicin (DOX) and Simvastatin (Sim) were purchased from Dalian Meilun Biotechnology Co., Ltd. (Dalian, China), 1,1'-Dioctadecyl-3,3,3',3'-tetramethylindotricarbocyanine iodide (DiR) was obtained from AAT Bioquest Inc (Sunnyvale, CA, USA). The Micro BCA protein assay kit was obtained from the Beyotime Institute of Biotechnology (Haimen, China). The 3-(4,5-dimethylthiazol-2-yl)-2,5-diphenyltetrazolium bromide (MTT), and cocktail protease inhibitor were purchased from Sigma Aldrich Co., Ltd (St. Louis, USA). Coumarin-6 was obtained from J&K Scientific Ltd (Shanghai, China). Soybean phosphatidylcholine (SPC), cholesterol, and DSPE-PEG_{2000}-NHS were purchased from Advanced Vehicle Technology Co., LTD (Shanghai, China). Annexin V-FITC Apoptosis Detection Kit was acquired from Invitrogen. Fetal bovine serum (FBS) and F12K medium were purchased from Thermo Fisher Scientific (Waltham, USA). Anti-VEGF antibody, anti-VEGFR2, β-Actin antibody, anti-caspase3 antibody, anti-LC3 antibody and anti-GAPDH antibody were purchased from CST Co., Ltd. (Boston, USA). All other reagents were of analytical grade from Sinopharm Chemical Reagent Co., Ltd. (Shanghai, China).

Cell lines and animals

The PCa cell line PC3 and HUVEC (Human Umbilical Vein Endothelial Cells) were obtained from the Center for Cell Line Resources, Chinese Academy of Sciences (Beijing, China). Male BALB/c nude mice (4 weeks old) were purchased from Shanghai SLAC Laboratory Animal Co., Ltd. (Shanghai, China).

Preparation of liposomes

Liposomes were prepared by the thin-film hydration method. The ratio of the lipid mixture of SPC, cholesterol, and DSPE-PEG_{2000}-NHS was 35:2.5:2 (w/w/w), and the drug ratio of DOX and Sim was 0.5:1 (w/w). All reagents were dissolved in chloroform. The organic solvents

were removed using a rotary evaporator in a 42°C water bath. The lipid film was hydrated with a 5% glucose solution, followed by ultrasonic treatment in water bath. Then suspensions were extruded through a 200 nm polycarbonate membrane with a liposome extruder (Avanti Polar Lipids, Alabaster, AL, USA). The un-encapsulated DOX and Sim were removed using a Sephadex G-50 column. The Herceptin-modified liposomes (termed H-Lip) were obtained by adding Herceptin to the liposomes at a molar ratio of 1:1, with incubation for 24 h at 4°C. The PEGylated liposomes without Herceptin (termed Lip) were used as the control.

Characterization of liposomes and drug loading

Particle size was measured by the Zeta Size Nanoparticle Analyzer (Malvern, UK). The morphology of the liposomes was investigated by transmission electron microscopy (TEM) after the samples were deposited on a copper grid and stained with 1% uranyl acetate. The DOX concentration in liposomes was determined by a fluorometer (λex 485 nm and λem 590 nm). Meanwhile, the concentration of Sim was detected by high-performance liquid chromatography (HPLC) equipped with the Diamonsil C18 column (250 mm × 4.6 mm, 5 μm). The mobile phase was 0.025 mol/L sodium dihydrogen phosphate solution (adjust pH value to 4.5 with phosphoric acid or sodium hydroxide test solution) - acetonitrile (35:65) with a flow rate of 1 mL/min, and detection λ of 238 nm. The drug loading capacity (LC) was calculated using the following equation: LC = Weight of encapsulated drugs/Weight of equivalent dried liposomes × 100% (1). The drug encapsulation efficiency (EE) was calculated by the following equation: EE = Weight of encapsulated drugs/Weight of total amount drugs × 100% (2).

In vitro stability and drug release assay of liposomes

Liposome stability was evaluated for 12 d at 4°C by measuring the changes in particle size. The *in vitro* drug release was conducted using a dialysis method. The free drug and liposomes were placed into a dialysis tube (MWCO 14 kDa), and dialyzed in phosphate-buffered saline (pH 7.4 containing 0.5% Tween 80 at 37°C in a shaker [120 rpm]). Drug concentrations were measured at varying time points. Experiments were performed in triplicate.

In vitro cellular uptake assays

The cells were seeded in a 12-well plate and cultured for 24 h. Then cells were treated with Coumarin-6-labeled Lip and H-Lip for 1 h incubation at the same concentration. The cells were thoroughly washed with PBS three times. Fluorescent images were obtained using the Zeiss Axio Observer Z1 fluorescence microscope. For quantitative measurement, the cellular uptake efficiency was determined using a flow cytometer (BD Pharmingen, San Jose, CA, USA).

In vitro cytotoxicity and apoptosis

Cell viability was measured using the standard Cell Counting Kit-8 (CCK-8) assay. Briefly, the PC3 cells were plated into 96-well plates at a density of 6×10^3 cells per well for overnight incubation. The blank liposomes, free DOX/Sim combination, Lip, and H-Lip were added to the cells and cultured for 48 h. CCK-8 solution (10 μL) was added to each well, and the cells were incubated for another 2 h. The absorbance was measured at 450 nm with a microplate reader. The cell viability was calculated using the following formula:

$$\text{Cell viability (\%)} = \frac{OD_{test} - OD_{blank}}{OD_{control} - OD_{blank}} \times 100 \quad (3)$$

The cell apoptosis activity was measured by flow cytometry. The cells were seeded in a 12-well plate and cultured for 24 h. Then the cells were exposed to the drugs (DOX 0.2 μg/mL, Sim 0.4 μg/mL, free DOX/Sim combination, and the liposomes at a dose equal to 0.2 μg/mL DOX and 0.4 μg/mL Sim), with subsequent incubation for 24 h. The cells were collected and washed with PBS three times and stained with the Annexin V-FITC Apoptosis Detection Kit according to the manufacturer's protocol. After transfection, cells were harvested, washed with PBS, and stained with Annexin V-FITC and propidium iodide according to the manufacturer's protocol. Fluorescence was analyzed by a flow cytometer.

Measurement of intracellular levels of reactive oxygen species

The PC3 cells were seeded in a 12-well plate at a density of 5×10^5 cells per well and cultured

for 24 h. The cells were treated with free drugs or the liposomes (equal to 0.2 μg/mL DOX or/and 0.4 μg/mL Sim) for 24 h. Then the cells were collected and stained with the Reactive Oxygen Species Detection Kit (Beyotime, Beijing, China) according to the manufacturer's protocol, and measured by flow cytometry.

Preliminary mechanisms underlying the combination therapy

Neovessels are significant factors for tumor growth because they can supply nutrients for tumors. In angiogenic signaling, VEGF is an angiogenic factor and its receptor, VEGFR2, is the predominant mediator [27]. To investigate the anti-tumor mechanisms of the combination therapy, the endothelial cell tube formation assay was conducted. Human umbilical vein endothelia cells (HUVECs) were seeded at a density of 5×10^4 cells per well onto a 24-well plate pre-treated with 60 μL 1% (w/v) Matrigel Matrix (Corning, NY, USA), and treated with free drugs or the liposomes (equal to 0.2 μg/mL DOX or/and 0.4 μg/mL Sim) for 16 h. Endothelial cell tube formation was observed by the Zeiss Axio Observer Z1 fluorescence microscope in the bright field. The cells were seeded in a 12-well plate, treated with drugs as above, and incubated for 24 h. Then the expression of VEGFR2 on HUVEC cells and VEGF on PC3 cells was analyzed by Western blotting. The tumor expression of CD-31, a marker of neovessels, was analyzed by immunohistochemistry.

Detection of autophagy levels

The PC3 cells were seeded in a 12-well plate at a density of 5×10^5 cells per well and cultured for 24 h. The cells were treated with free drugs or the liposomes (equal to 0.2 μg/mL DOX or/and 0.4 μg/mL Sim) for 24 h. Then the cells were collected and incubated with RIPA lysis buffer (Beyotime). Microtubule-associated protein 1A/1B-light chain 3 (LC-3) levels were determined by Western blotting with an anti-LC3 antibody. After staining with detection reagent (Thermo Fisher Scientific, Waltham, MA, USA) gel imaging analysis (ChemiDoc MPTM Imaging System; Bio-Rad, Hercules, CA, USA) was performed.

In vivo imaging

The subcutaneous PC3 tumor model was developed by injection of 3×10^6 cells into the backs of the nude mice. The subcutaneous tumor-bearing mice were injected with Lip@DiRs or H-Lip@DiRs via the tail vein. The biodistribution of nanoparticles was monitored using the IVIS imaging system (Caliper PerkinElmer, Hopkinton, MA, USA) at different time points. At the end of the experiment, mice were sacrificed, and the tumors and major organs (heart, liver, spleen, lung, kidney) were harvested for *ex vivo* imaging. Images and regions of interest (ROI) were processed using Spectrum Living Image 4.0 software.

In vivo treatment

The tumor sizes in subcutaneous PC3 tumor-bearing mice were approximately 100 mm^3; mice were randomly assigned to six groups (n = 5). Saline, free DOX/Sim combination, Lip, or H-Lip (at a same dose of 1 mg/kg DOX and 2 mg/kg Sim) were injected via the tail vein every 2 d over a period of 20 d. The body weight and tumor volume were monitored throughout the study, and the latter was estimated using the following formula: $V = L \times W^2/2$ (L-tumor's length W-tumor's width) (4).

At the experimental endpoint, the tumors and the main organs were dissected and weighed. The tumor inhibition rates were calculated by tumor weight. The main organs were fixed for 48 h in 4% paraformaldehyde for histopathological examination to assess any side effects. To assess the *in vivo* induction of apoptosis, TdT-mediated dUTP nick end labeling technique (TUNEL) staining was performed.

Statistical data analysis

Data are presented as the mean ± standard deviation (SD) for results obtained from three independent trials unless otherwise indicated. Statistical analysis was performed using Origin 9.0. Statistical significance was evaluated using Student's t-test. Differences were considered significant at $P < 0.05$.

Results and discussion

Physical characterization of liposomes

Herceptin is a promising targeting ligand, as it is a monoclonal antibody used to treat cancers and is easily conjugated to DSPE-PEG_{2000}-NHS. The mean hydrodynamic diameter of Lip and H-Lip in PBS buffer at pH 7.4 was 129 ± 4 nm

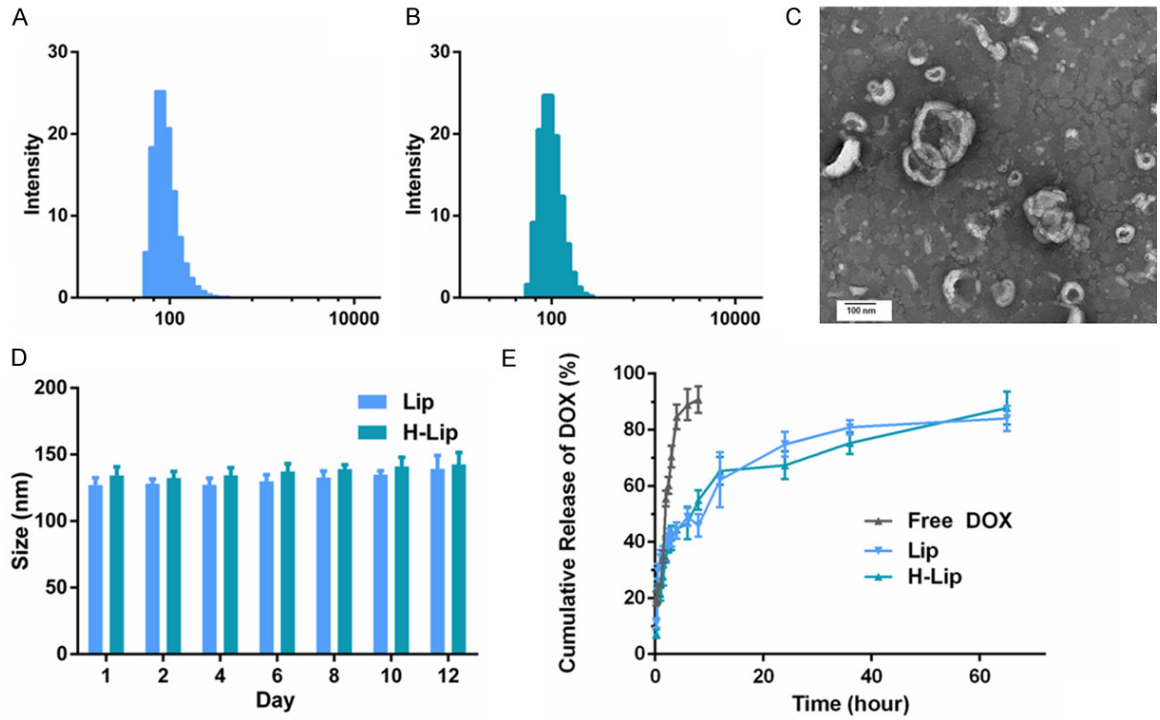

Figure 1. Characterization of liposomes. A. Size of Lip. B. Size of H-Lip. C. Transmission electron microscopy image of H-Lip. Scale bar: 100 nm. D. Changes in liposome size at PBS (pH = 7.4). E. *In vitro* release of profiles of DOX at various intervals.

Table 1. The LC% and EE% of Lips and H-Lips

	Lip	H-Lip
EE of DOX (%)	81.48 ± 2.55	84.32 ± 4.21
EE of Sim (%)	80.14 ± 3.75	81.7 ± 1.53
LC of DOX (%)	0.96 ± 0.03	1.0 ± 0.05
LC of Sim (%)	1.81 ± 0.18	1.89 ± 0.08

(polydisperity index PDI: 0.07 ± 0.02), 134 ± 5 nm (PDI: 0.08 ± 0.01), respectively (**Figure 1A**, **1B**), suggesting that there was a slight increase in size with treatment of Herceptin. Transmission electron microscopy was also used to visualize the morphology of H-Lip, which displayed a spherical shape with a diameter of about 130 nm (**Figure 1C**). Moreover, prior experiments showed that the spherical shape of the nanoparticles could enhance cellular uptake via endocytosis compared to the needle shape [26]. The stability of drug-liposomes at different storage times was tested by measuring the changes in size and PDI. Within a storage period of 12 days in PBS (pH 7.4), the particle size of the liposomes only underwent minor changes, increasing from about 135 nm to almost 144 nm (**Figure 1D**). This result demonstrated the stability of Lip and H-Lip in physiological conditions within 12 days. Drug loading content plays an important role in the formulation of drug delivery system and directly affects the therapeutic effects of the system. The drug loading content (LC%) and encapsulation efficiency (EE%) of Sim in H-Lip was almost 1.81% and 81.7%, respectively. The DOX loading content herein is lower, the LC% was 1%, and the EE% was around 84.32%. The EE% and LC% of the Lip, H-Lip were similar (**Table 1**).

To increase the affinity between liposomes and PC3 cells, the DSPE-PEG_{2000}-NHS that used in H-Lip was modified by Herceptin. To evaluate the amount of DOX released from Lip and H-Lip at different time intervals *in vitro*, PBS with 0.5% (w/v) Tween 80 at pH 7.4 was selected as the release media to simulate the pH values of the physiological environment. The release profiles of DOX *in vitro* were represented by the percentage of DOX release with respect to the amount of DOX loading in the liposomes (**Figure 1E**). Both liposomes underwent burst release from 0.25 to 0.5 h, due to the release of drug molecules near the interface [28]. Sustained

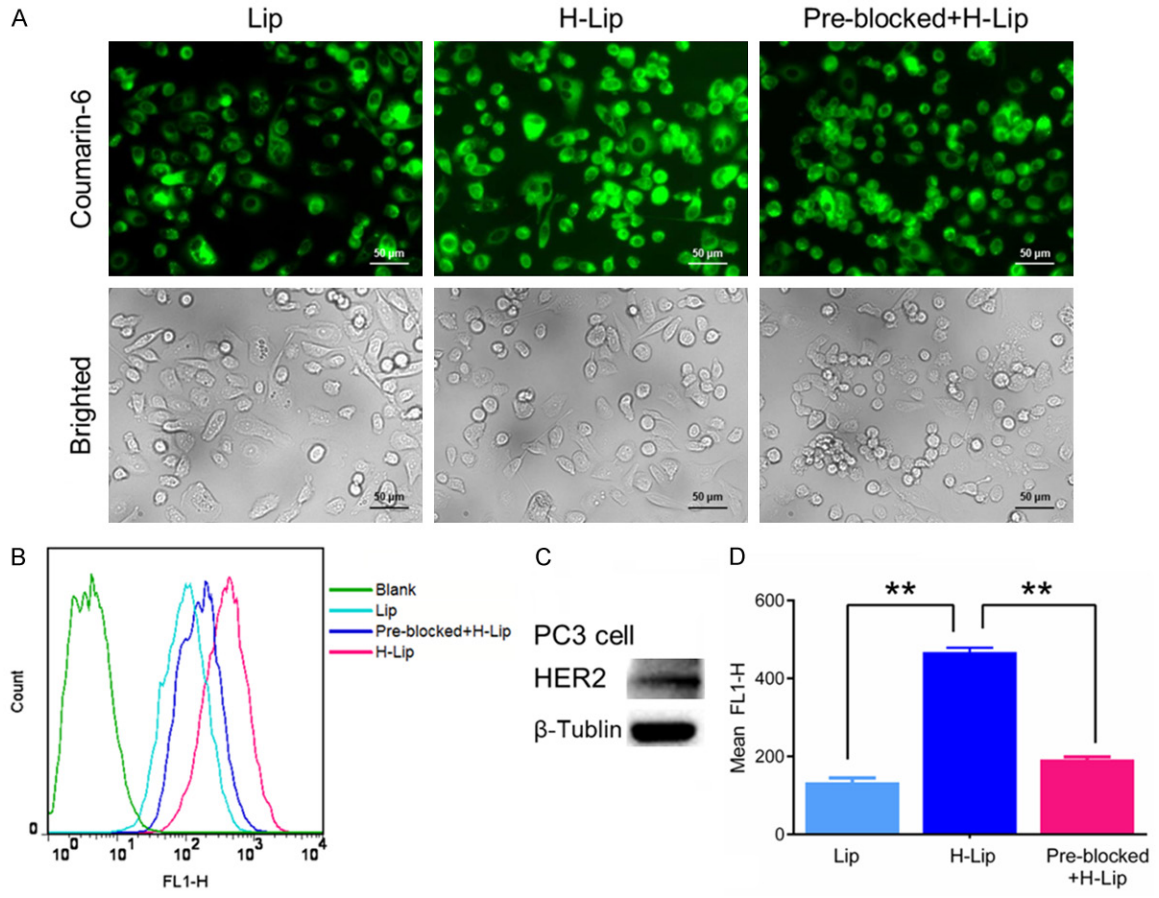

Figure 2. Cellular uptake of the liposomes. A. Fluorescence images of the cells treated with liposomes. Scale bar: 50 μm. B. Flow cytometry analysis of the uptake efficiency of the liposomes. C. HER-2 expression in the tumor cells. D. Quantitative analysis of fluorescence intensity. The statistically significant difference was defined as *P < 0.05, **P < 0.01, and ***P < 0.001.

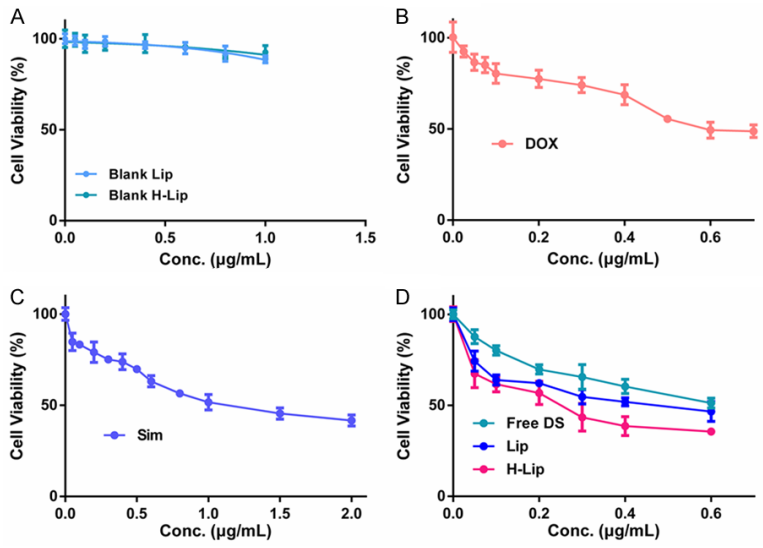

Figure 3. Anti-tumor effect in vitro. A. Cytotoxicity test of blank liposomes. B. Cytotoxicity test of free DOX. C. Cytotoxicity test of free Sim. D. Cytotoxicity test of free DOX-Sim combination, Lips, H-Lips.

and controlled drug release could be beneficial to anticancer therapy by preventing cancer cells from acquiring drug resistance [29].

Cellular uptake of liposomes

To investigate the cellular uptake ability of liposomes, coumarin-6 labeled liposomes were incubated with the PC3 cells for 1 h, after which coumarin-6 (green) could be clearly observed in the cells. Fluorescent imaging showed more intense cellular uptake when cells were treated with H-Lip than with Lip (**Figure 2A**). In accordance with the confocal microscopy results, a

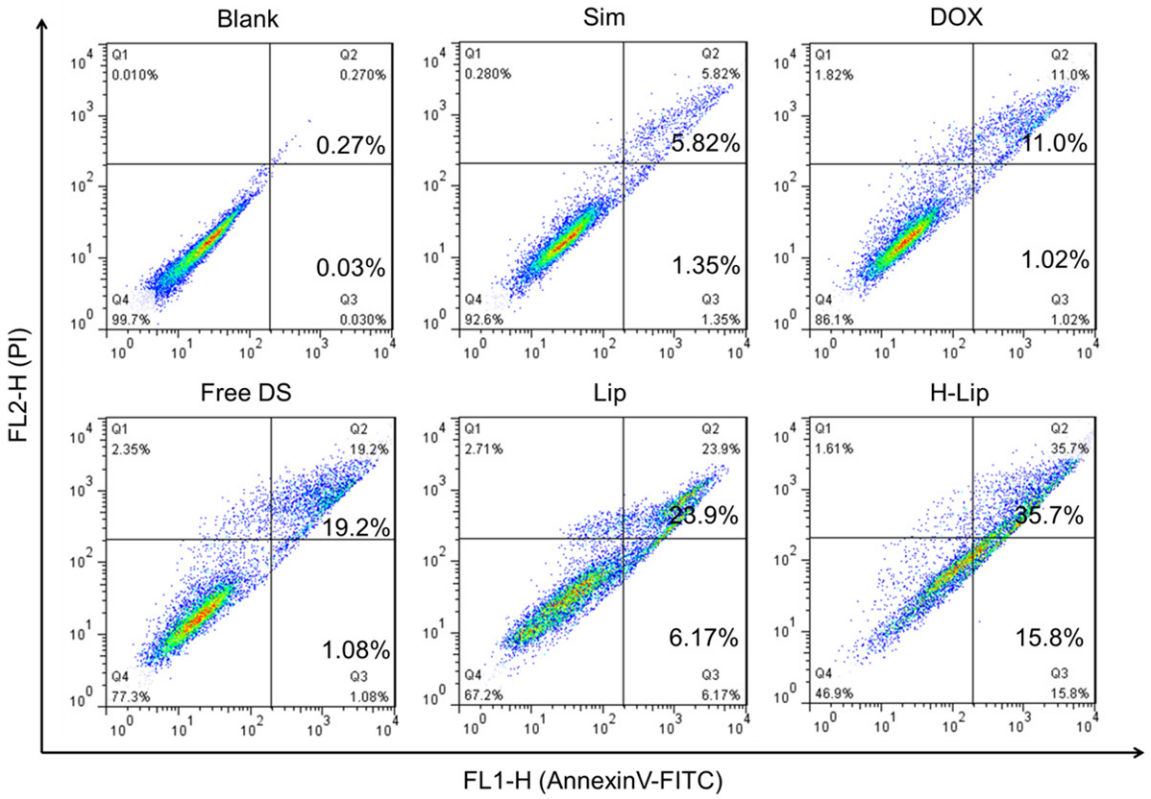

Figure 4. Apoptosis assay of the liposomes.

flow cytometry curve of H-Lip showed an obvious right shift, indicating the clear increase of cell fluorescence after incubation with H-Lip compared to Lip (**Figure 2B**). Meanwhile, H-Lips resulted in a significant increase (3.5-fold) of cellular uptake compared to non-targeted liposomes, indicative of the targeting effects of Herceptin *in vitro*. To assess the role of Herceptin in the cellular uptake of H-Lip, uptake was also tested in Herceptin (+) containing medium. As shown in **Figure 2D**, when the HER-2 receptor was pre-incubated with free Herceptin, the uptake of H-Lip was inhibited (> 41%). Western blot analysis showed that the expression level of HER-2 was increased in PC3 cells (**Figure 2C**), thereby revealing that modification with Herceptin was an effective approach for delivering liposomes to PC3 cells via Herceptin-HER-2 affinity. This PC3 targeting property may reduce the cytotoxicity of drugs in normal cells.

In vitro antitumor activity of liposomes

To investigate the chemotherapeutic effects of liposomes and the DOX-Sim combination *in vitro*, PC3 cell viability was measured using the Cell Counting Kit-8 (CCK-8) after drug treatment for 48 h in the presence and absence of DOX and/or Sim. As can be seen in **Figure 3A**, blank liposomes had no obvious cytotoxicity in PC3 cells. In case of free drugs, the IC_{50} value of free single DOX and free single Sim were 0.74 μg/mL, 1.21 μg/mL respectively, while in the case of drug combination, the IC_{50} value of free DOX/Sim combination group, Lips, H-Lips were 0.67 μg/mL, 0.46 μg/mL, 0.22 μg/mL, respectively. This is the concentration of doxorubicin, because the concentration of the Sim is fixed. This was mainly due to the synergistic anti-proliferative effects between these two components. Notably, the cytotoxicity assay showed that both liposomes had higher cytotoxicity than the free DOX-Sim combination (**Figure 3**). The H-Lip targeting co-delivery system showed enhanced induction of cell proliferation (cell viability of 53.3%), which was most likely due to the efficient cellular uptake. The results were in agreement with our cellular uptake experiments. The results of the cell viability test demonstrated that H-Lip had clear inhibition effects on PC3 cells; thus, we decided to determine if the designed liposomes would lead to the induction of apoptosis. In the following, the apoptosis results show a similar

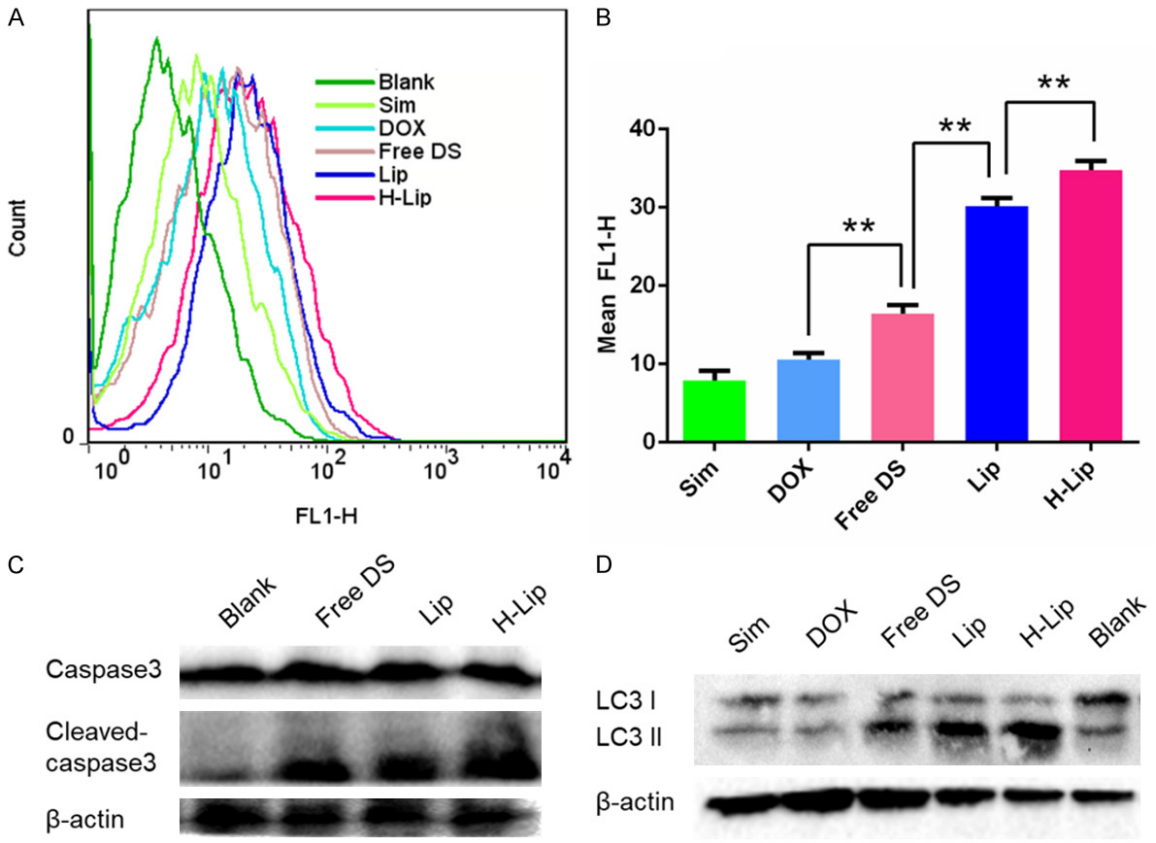

Figure 5. Study on the mechanisms of the liposomes. A. Flow cytometry analysis of intracellular levels of ROS. B. Quantitative analysis of fluorescence intensity. C. Western blotting of caspase-3 expression. D. Western blotting analysis of autophagy expression in PC3 cells. The statistically signifigcant difference was analysised by student t-test and defined as *P < 0.05, **P < 0.01, and ***P < 0.001.

trend. Cell apoptosis was analyzed using the Annexin V-FITC Apoptosis Detection Kit. As shown in **Figure 4**, the apoptotic rates (early and late) were 7.17%, 12.02%, 20.28%, 30.7%, and 51.5% for free Sim, free DOX, free DOX-Sim combination, Lip, and H-Lip, respectively. More apoptotic cells were detected in H-Lip than in the other groups. ROS production is a major mechanism for apoptosis induced by antineoplastic drugs [30]. The intracellular ROS levels were measured by an ROS detection kit. As shown in **Figure 5A** and **5B**, drug combination significantly increased intracellular ROS levels. H-Lip had the highest levels of ROS compared to other groups with statistical significance. To evaluate the effects of liposomes on apoptosis, the expression of pro-apoptotic markers was determined by Western blotting. The expression level of procaspase-3 is widely accepted to play a key role in the caspase family-related apoptotic cascade [30-32]. After treatment with H-Lip, the expression level of procaspase-3 was dramatically decreased, while there were much higher levels of cleaved caspase 3, representing early apoptosis (**Figure 5C**). These data indicated the activation of caspase-3, which catalyze the hydrolysis of many protein substrates for cell apoptosis. Some studies have shown that chemotherapy drugs are able to induce autophagic cell death, and the autophagosome-associated protein LC3 is the most commonly monitored autophagy-related biomarker [33]. Western blot analysis showed that the combination of DOX and Sim induced obvious autophagy in PC3 cells, and the highest level of LC3 was seen in the group treated with H-Lip (**Figure 5D**). These results were consistent with those from the CCK-8 assay, indicating the synergistic effects between DOX and Sim.

Biodistribution of liposomes

The use of Herceptin as target receptor for the delivery of DOX and Sim to prostate cancer cells is a promising approach, as demonstrated

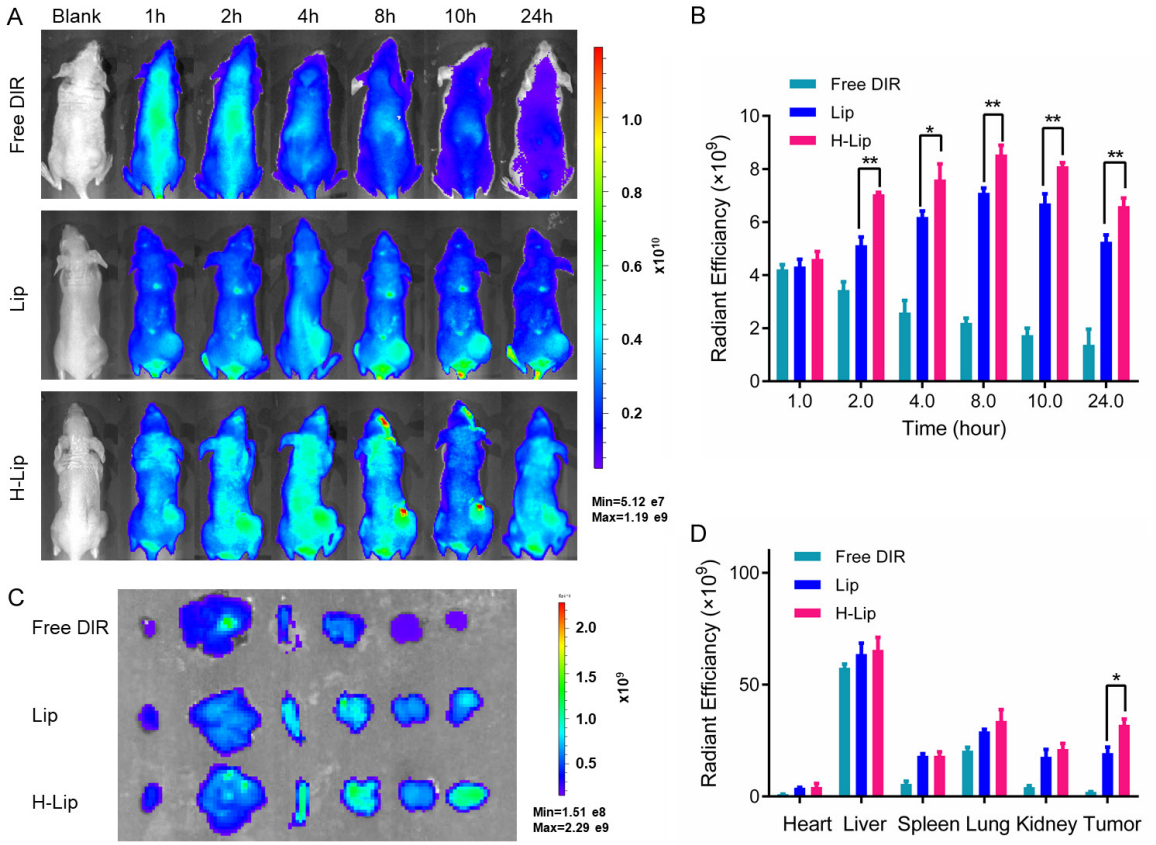

Figure 6. Bio-distribution of liposomes in tumor model. A. Whole body imaging from 1 to 24 h. B. *In vivo* radiant efficiency at the tumor sites. C. *Ex vivo* imaging of the major organs dissected from the mice. D. *Ex vivo* radiant efficiency of the tumors. The statistically significant difference was analysised by student t-test and defined as *P < 0.05, **P < 0.01, and ***P < 0.001.

by the cellular uptake results. Next, the tumor targeting efficiency of the liposomes *in vivo* was investigated. The nude mice bearing PC3 human prostate cancer xenografts were established to estimate the biodistribution and tumor selectivity characteristics of liposomes with or without Herceptin modification. DIR was used as the model drug. After being injected intravenously via the tail vein of mice, the fluorescence at the tumor site was observed within 1 h. Subsequently, the fluorescent intensity at the tumor site was gradually increased, and peaked at 8 h. Real-time *in vivo* imaging showed higher fluorescent intensity at the tumor site in the H-Lip group compared to the Lip group (**Figure 6A**, **6B**) e.g., the tumor uptake of H-Lip was 8.5 × 10^9 at 8 h and 6.6 × 10^9 at 24 h, which was comparable with that of Lip (7.1 × 10^9 at 8 h and 5.25 × 10^9 at 24 h) within experimental error. In contrast, the tumor uptake of free DIR was only 2.2 × 10^9 at 8 h and was 1.3 × 10^9 at 24 h in the same model. PEG-modified liposomes can stay in tumors for a long time due to their long half-life and mean residence time. Immediately at the end of the *in vivo* imaging, the animals were sacrificed, and the major organs and tumors were harvested and imaged. Imaging of the dissected tissues showed higher tumor accumulation in the H-Lip group (**Figure 6C**, **6D**). Although tumors treated with targeting or non-targeting liposomes had strong fluorescence, for comparison purposes, we evaluated the ROI in the H-Lip group and found that it was greater that of Lip and free DIR. These data reveal the enhanced tumor delivery in PC3 tumors *in vivo*, as aided by Herceptin-mediated targeting.

In vivo anti-tumor efficacy

To determine the therapeutic effects of H-Lip on prostate cancer *in vivo*, nude mice were implanted with PC3 cells and used for therapeutic efficacy evaluation. The DOX/Sim combi-

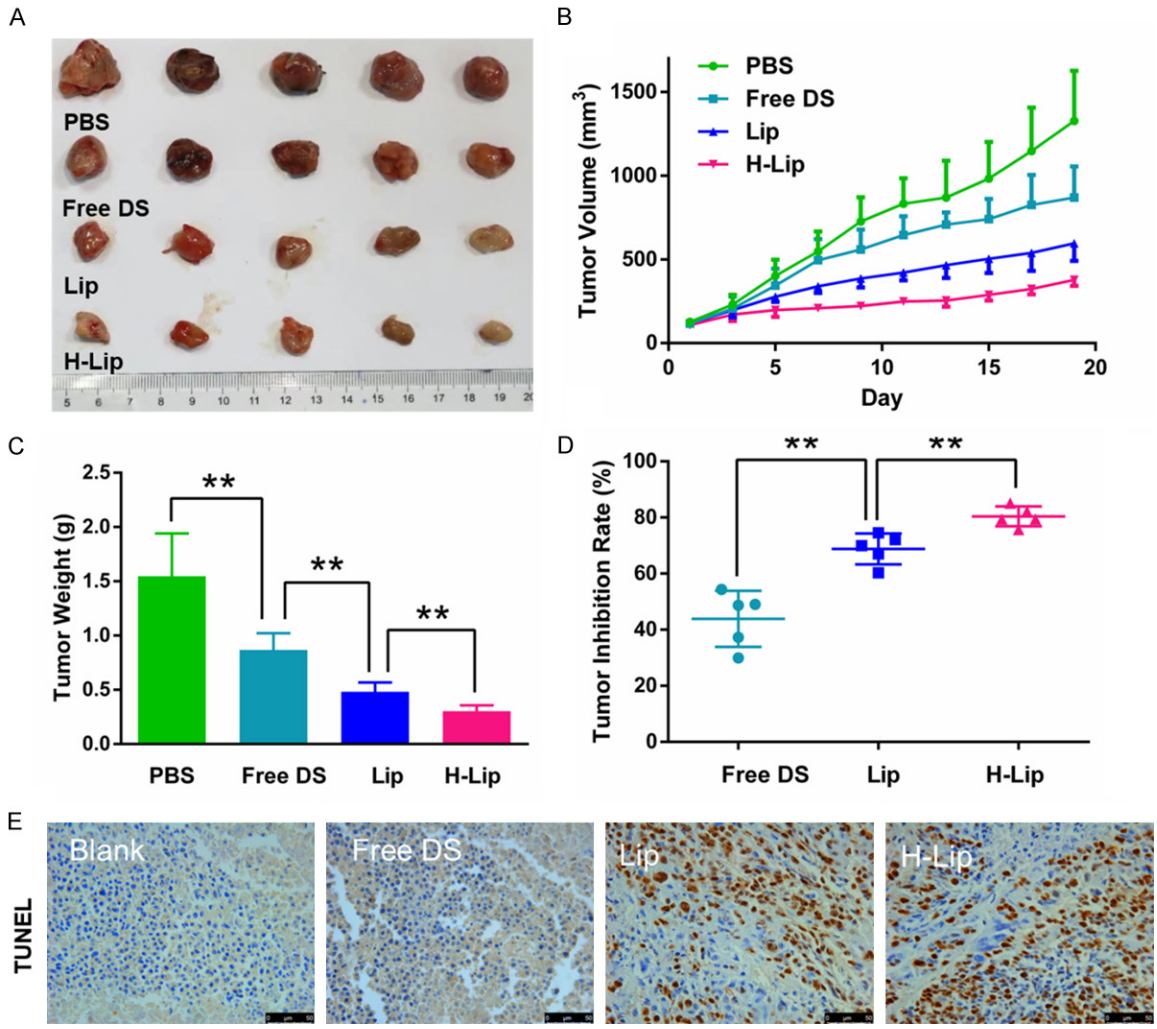

Figure 7. Antitumor efficacy. Anti-tumor effects of nude mice bearing PC3 cancer cells xenografts. Groups were treated every 2 days (total 10 doses). Free DS = DOX-Sim solution, Lip = non-targeting liposome with the two drugs, H-Lip = targeting liposome with the two drugs. A. Photographs of tumor tissues obtained at the end of pharmacological experiment. B. Tumor growth curve. C. Tumor weight at the endpoint. D. Tumor inhibition rate. E. TUNEL assay of apoptosis in tumors. The statistically significant difference was analysised by student t-test and defined as *P < 0.05, **P < 0.01, and ***P < 0.001.

nation in solution, liposomes, and targeting liposomes were evaluated. As expected, at the experimental endpoint, the dissected tumors were weighed and displayed a similar trend as the tumor volume. The targeting liposomes containing co-loaded DOX and Sim efficiently inhibited tumor growth and displayed the best antitumor activity among all of the treatment groups with statistical significance. Treatment with Lip and H-Lip at a dose of DOX 1 mg/kg and Sim 2 mg/kg resulted in significant tumor shrinking with an inhibition rate of 68.77% and 80.36%, respectively, while that of the group receiving free DOX/Sim combination was 43.82% (**Figure 7A-D**). The H-Lip group was more effective in controlling tumor growth compared to the non-targeting Lip due to HER-2 receptor expression in the prostate tumors, causing Herceptin-modified liposomes to target PC3 cells. These data were in agreement with the results of the cell viability study, which showed synergistic efficacy of DOX/Sim co-delivery, as well as the enhanced cellular uptake in PC3 cells. The TUNEL results showed that H-Lip had the highest apoptosis rate in the tumor, and that Lips displayed superiority over the free DOX/Sim combination (**Figure 7E**). The body weight of the animals was recorded throughout the experiment (**Figure 8A**), and no obvious weight loss was observed, indicating

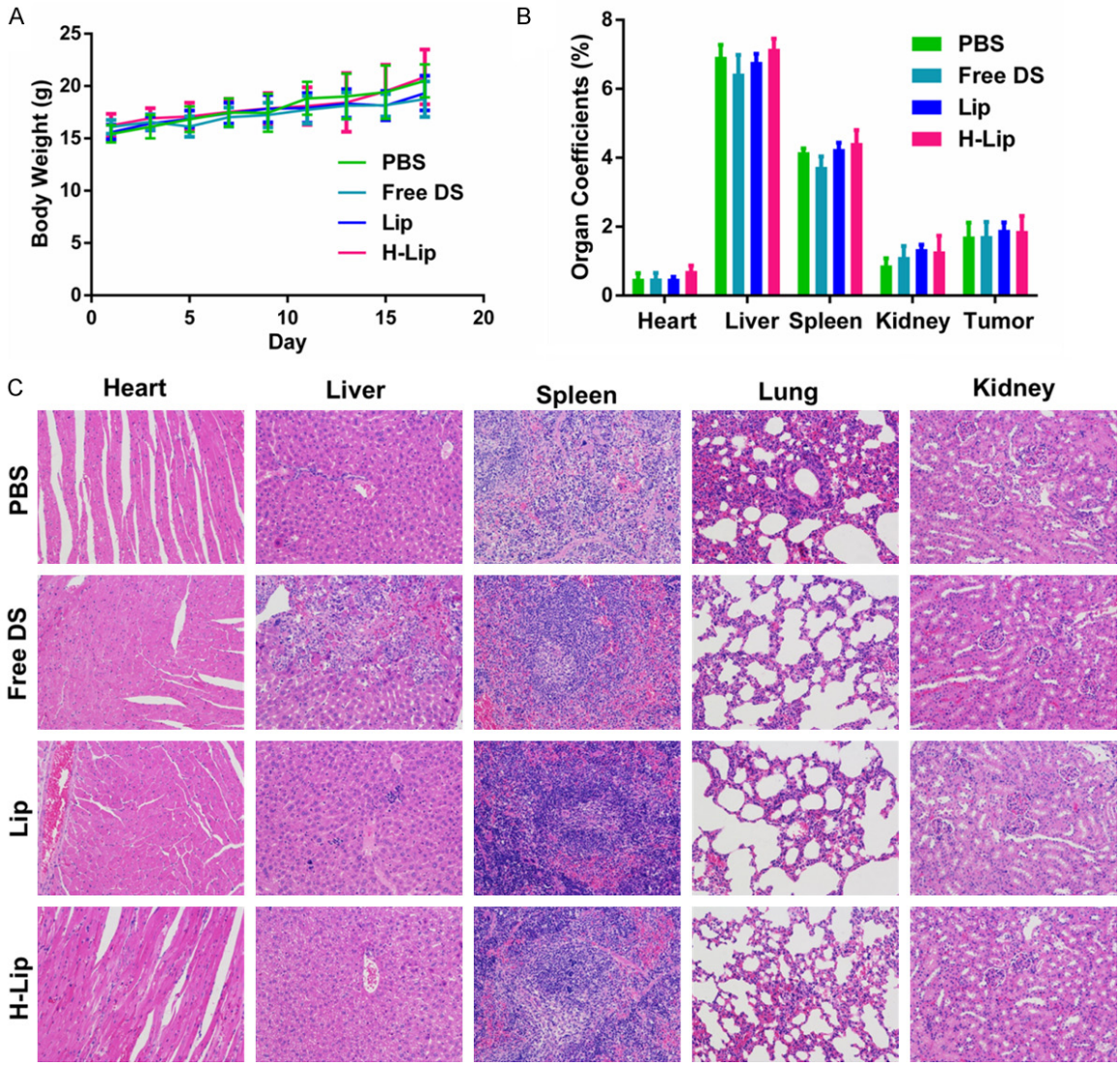

Figure 8. Evaluation of toxic and side effects. A. Changes in body weight during the course of treatment. B. Organ coefficients. C. H&E staining of major organs after treatment.

minor toxicity. Hematoxylin and eosin staining showed that there were no visible lesions in the major organs, suggesting that there were no significant toxic side effects caused by drug treatment (**Figure 8C**). Moreover, treatment did not cause significant changes in organ weight coefficient (**Figure 8B**). Therefore, liposomal drug delivery of DOX and Sim is a bio-safe co-delivery system for the treatment of prostate cancer.

Preliminary study of related synergistic mechanisms

To gain deeper insights into the anti-cancer mechanisms, angiogenesis-related experiments were conducted to monitor the possible mechanisms. Angiogenesis is a key driving factor for tumor proliferation. VEGF-A (also referred to as VEGF) is the most potent angiogenic factor, and its receptor, VEGFR2, is the predominant mediator of angiogenic signaling [34]. Our results demonstrated that HUVEC tube formation on the Matrigel Matrix was obviously inhibited with different treatments (**Figure 9A**), and as shown in **Figure 9B**, Vascular Endothelial Growth Factor Receptor 2 (VEGFR2) expression was downregulated after drug treatment compared. We also found that H-Lip could decrease the expression of VEGF in tumor cells (**Figure 9C**). Thus, the combination of DOX

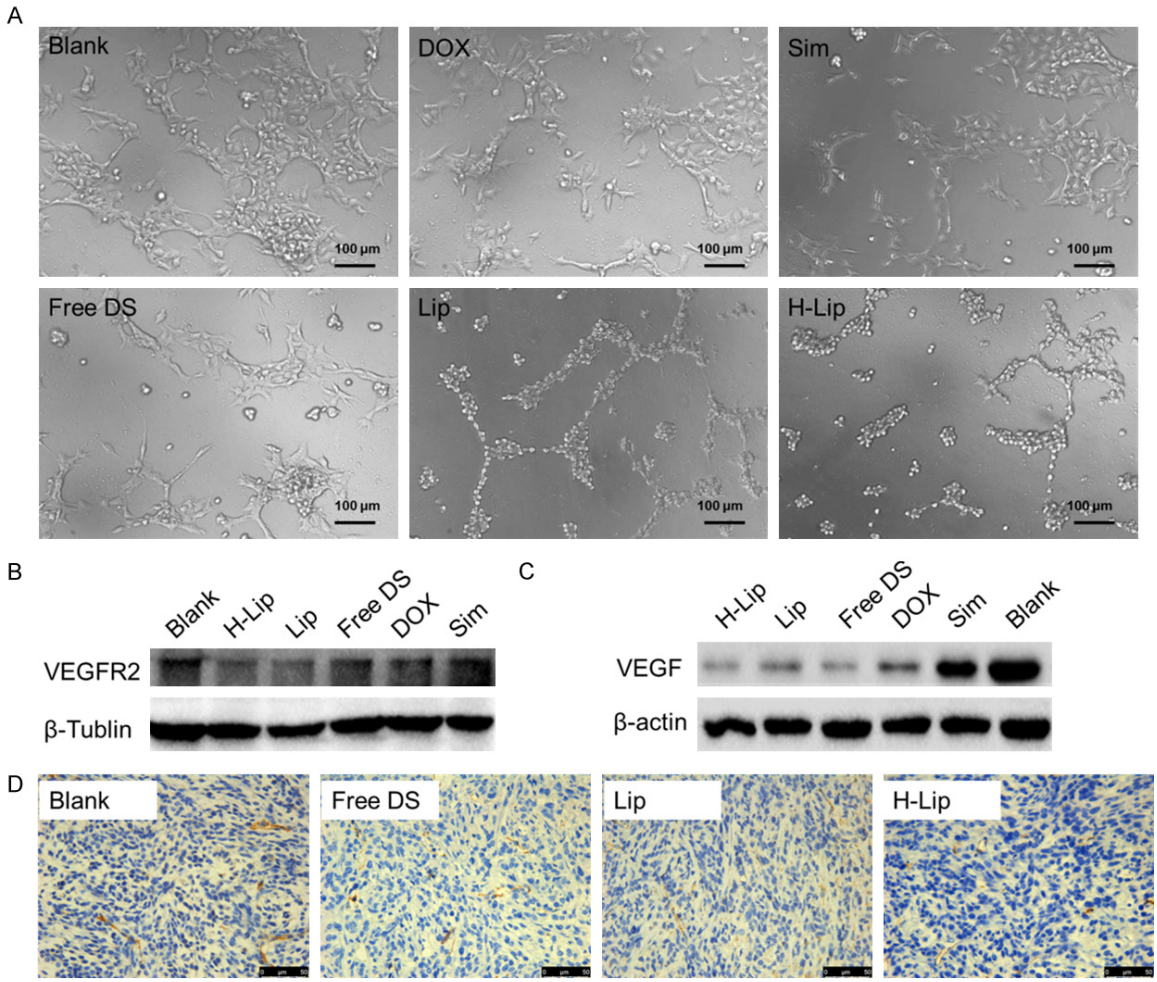

Figure 9. Mechanistic study. A. Vascular endothelial cell tube formation on the Matrigel Matrix. Scale bar, 100 μm. B. VEGFR2 protein expression in HUVECs after treatment with different liposomes. C. VEGF protein expression in tumor tissues measured by Western blotting. D. Investigation of tumor-associated blood vessels using anti-CD31 immunohistochemical staining (brown).

and Sim was effective in targeting VEGF and reducing angiogenesis. To further investigate the anti-angiogenesis effects, we performed immunohistochemistry staining using anti-CD-31 on sections of tumor tissue that received different treatments. The vessel number in the H-Lip group was clearly less than that in the other groups (**Figure 9D**). The combination therapy led to synergistic anti-angiogenesis, demonstrating that inhibition of angiogenesis was an anti-tumor mechanism of this combination therapy.

Statistical analyses

All data were analyzed by GraphPad Prism 6 software. The results were shown as mean ± SD ($n > 3$). The statistical analysis was performed by Student's t-test and one-way ANOVA. The statistically significant difference was defined as $^*P < 0.05$, $^{**}P < 0.01$, and $^{***}P < 0.001$.

Conclusions

In this study, we successfully formulated Herceptin-modified liposomes containing co-entrapped Sim and DOX as chemotherapeutic agents. This co-delivery system may provide a possible adjuvant therapy for prostate cancer. The physiochemical properties, release behaviors, bio-distribution, possible mechanisms of this co-delivery system, the interaction between this delivery system and targeted PC-3 cells, and their toxicity to tumors were explored. First, we demonstrated that the Herceptin ligand

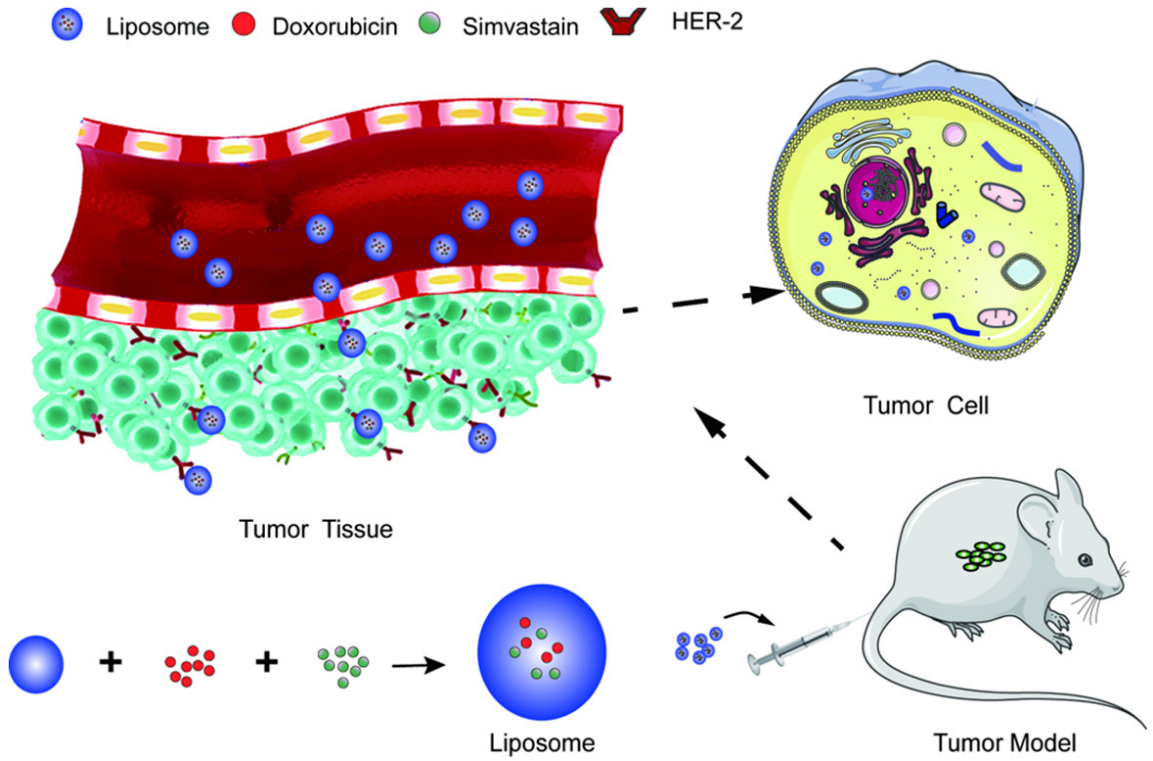

Scheme 1. The co-delivery system for Prostate cancer (PCa).

could bind to prostate cancer cells via HER-2 receptors, and the delivery vectors were effectively taken up by the cancer cells. Moreover, pre-cubed Herceptin inhibited binding of the targeted liposomes, confirming the involvement of Herceptin in the process of liposome targeting. Second, the combination therapy against cancer, via multiple mechanisms of enhanced intracellular ROS levels, apoptosis induction, cell autophagy promotion, and anti-angiogenesis demonstrated that the H-Lip significantly arrested the tumor growth. Thus, H-Lip may be a potential nanomedicine for controlling prostate cancer with the strategy of combination therapy using Sim and DOX. Our results show that this targeted drug delivery system has good potential for clinical translation due to its easy preparation process and therapeutic efficacy. Furthermore, extending carboxylic groups on the surface may link the delivery system to other targeting antibodies, resulting in selected targets and enhanced bioavailability. This strategy will facilitate the further development for multi-functional targeted drug delivery to augment therapeutic efficacy. Herceptin targeting may also be applicable to other HER-2-expressing tumors besides prostate cancer.

Acknowledgements

We are thankful for the support from Hangzhou Science and Technology Development Plan Project (20150633B15, 20150633B17), Zhejiang Natural Science Foundation Committee Project (Y18H160285), Zhejiang Medical Science and Technology Project (2019RC241) and Zhejiang Administration of Traditional Chinese Medicine Project (2017ZB070). And we would like to thank LetPub (www.letpub.com) for providing linguistic assistance during the preparation of this manuscript.

Disclosure of conflict of interest

None.

Address correspondence to: Huadong He, Department of Urology, Affiliated Hangzhou First People's Hospital, School of Medicine, Zhejiang University, Hangzhou 310006, China. Tel: +86-1315718944; E-mail: plumber19@163.com

References

[1] Zhu Y, Liu C, Armstrong C, Lou W, Sandher A and Gao AC. Anti-androgens inhibit ABCB1 efflux and ATPase activity and reverse docetaxel

resistance in advanced prostate cancer. Clin Cancer Res 2015; 21: 4133.
[2] Jemal A, Ma J, Siegel R, Fedewa S, Brawley O and Ward EM. Prostate cancer incidence rates 2 years after the us preventive services task force recommendations against screening. JAMA Oncol 2016; 2: 1657-1660.
[3] Howlader N, Noone AM, Krapcho M, Garshell J, Miller D, Altekruse SF, Kosary CL, Yu M, Ruhl J, Tatalovich Z, Mariotto A, Lewis DR, Chen HS, Feuer EJ, Cronin KA (eds). SEER Cancer Statistics Review, 1975-2012, National Cancer Institute. Bethesda, MD, https://seer.cancer.gov/archive/csr/1975_2012/, based on November 2014 SEER data submission, posted to the SEER web site, April 2015.
[4] Horwich A, Parker C, De RT, Kataja V; Group EGW. Prostate cancer: ESMO Clinical Practice Guidelines for diagnosis, treatment and follow-up. Ann Oncol 2013; 24 Suppl 6: vi106.
[5] Mottet N, Bellmunt J, Bolla M, Joniau S, Mason M, Matveev V, Schmid HP, Van dKT, Wiegel T and Zattoni F. [EAU guidelines on prostate cancer. Part II: treatment of advanced, relapsing, and castration-resistant prostate cancer]. Eur Urol 2011; 59: 572-583.
[6] Heidegger I, Massoner P, Eder IE, Pircher A, Pichler R, Aigner F, Bektic J, Horninger W and Klocker H. Novel therapeutic approaches for the treatment of castration-resistant prostate cancer. J Steroid Biochem Mol Biol 2013; 138: 248-256.
[7] Sartor O and Parker C. Re: novel therapies for metastatic castrate-resistant prostate cancer. J Natl Cancer Inst 2012; 104: 717; author reply 717.
[8] Feldman BJ and Feldman D. The development of androgen-independent prostate cancer. Nat Rev Cancer 2001; 1: 34-45.
[9] Kirby M, Hirst C and Crawford ED. Characterising the castration-resistant prostate cancer population: a systematic review. Int J Clin Pract 2011; 65: 1180-1192.
[10] Sartor O, Gillessen S. Treatment sequencing in metastatic castrate-resistant prostate cancer. Asian J Androl 2014; 16: 426-431.
[11] Utreja P, Jain S and Tiwary AK. Novel drug delivery systems for sustained and targeted delivery of anti-cancer drugs: current status and future prospects. Curr Drug Deliv 2010; 7: 152-161.
[12] Safwat S, Ishak RA, Hathout RM and Mortada ND. Statins anticancer targeted delivery systems: re-purposing an old molecule. J Pharm Pharmacol 2017; 69: 613-624.
[13] Hindler K, Cleeland CS, Rivera E and Collard CD. The role of statins in cancer therapy. Oncologist 2006; 11: 306-315.
[14] Bonovas S, Filioussi K and Sitaras NM. Statin use and the risk of prostate cancer: a metaanalysis of 6 randomized clinical trials and 13 observational studies. Int J Cancer 2010; 123: 899-904.
[15] Sun Q, Arnold RS, Sun CQ, Petros JA. A mitochondrial DNA mutation influences the apoptotic effect of statins on prostate cancer. Prostate 2015; 75: 1916-1925.
[16] Papadopoulos G, Delakas D, Nakopoulou L and Kassimatis T. Statins and prostate cancer: molecular and clinical aspects. Eur J Cancer 2011; 47: 819-830.
[17] Sekine Y, Nakayama H, Miyazawa Y, Kato H, Furuya Y, Arai S, Koike H, Matsui H, Shibata Y and Ito K. Simvastatin in combination with meclofenamic acid inhibits the proliferation and migration of human prostate cancer PC-3 cells via an AKR1C3 mechanism. Oncol Lett 2018; 15: 3167.
[18] You HB and Park K. Targeted drug delivery to tumors: myths, reality and possibility. J Control Release 2011; 153: 198-205.
[19] Vinoth-Kumar L. Therapeutic efficacy of nanomedicines for prostate cancer: an update. Invest Clin Urol 2016; 57: 21-29.
[20] Wilhelm S, Tavares AJ, Dai Q, Ohta S, Audet J, Dvorak HF and Chan WCW. Analysis of nanoparticle delivery to tumours. Nat Rev Mater 2016; 1: 16014.
[21] Elbayoumi TA and Torchilin VP. Tumor-targeted immuno-liposomes for delivery of chemotherapeutics and diagnostics. J Pharm Innov 2008; 3: 51-58.
[22] Le PC, Koumakpayi IH, Lessard L, Mes-Masson AM and Saad F. EGFR and Her-2 regulate the constitutive activation of NF-kappaB in PC-3 prostate cancer cells. Prostate 2010; 65: 130-140.
[23] Nahta R and Esteva FJ. HER-2-targeted therapy: lessons learned and future directions. Clin Cancer Res 2003; 9: 5078-5084.
[24] Uriarte-Pinto M, Escolano-Pueyo Á, Gimeno-Ballester V, Pascual-Martínez O, Abad-Sazatornil MR and Agustín-Ferrández MJ. Trastuzumab, non-pegylated liposomal-encapsulated doxorubicin and paclitaxel in the neoadjuvant setting of HER-2 positive breast cancer. Int J Clinl Pharm 2016; 38: 446-453.
[25] Eloy JO, Petrilli R, Chesca DL, Saggioro FP, Lee RJ and Marchetti JM. Anti-HER2 immunoliposomes for co-delivery of paclitaxel and rapamycin for breast cancer therapy. Eur J Pharm Biopharm 2017; 115: 159.
[26] Nguyen HT, Tran TH, Thapa RK, Phung CD, Shin BS, Jeong JH, Choi HG, Yong CS and Kim JO. Targeted co-delivery of polypyrrole and rapamycin by trastuzumab-conjugated liposomes for combined chemo-photothermal therapy. Int J Pharm 2017; 527: 31-71.
[27] Holderfield MT, Hughes CC. Crosstalk between vascular endothelial growth factor, notch, and

transforming growth factor-beta in vascular morphogenesis. Circ Res 2008; 102: 637.
[28] Loverde SM, Klein ML and Discher DE. Nanoparticle shape improves delivery: rational coarse grain molecular dynamics (rCG-MD) of taxol in worm-like PEG-PCL micelles. Adv Mater 2012; 24: 3823-3830.
[29] Abbasi AZ, Prasad P, Cai P, He C, Foltz WD, Amini MA, Gordijo CR, Rauth AM and Wu XY. Manganese oxide and docetaxel co-loaded fluorescent polymer nanoparticles for dual modal imaging and chemotherapy of breast cancer. J Control Release 2015; 209: 186-196.
[30] Morrison BW, Doudican NA, Patel KR and Orlow SJ. Disulfiram induces copper-dependent stimulation of reactive oxygen species and activation of the extrinsic apoptotic pathway in melanoma. Melanoma Res 2010; 20: 11.
[31] Yang TJ, Haimovitz-Friedman A and Verheij M. Anticancer therapy and apoptosis imaging. Exp Oncol 2012; 34: 269.
[32] Zhang J, Di W, Zhen X, Liang S, Han H, Hui S, Yan Z, Yan Y and Li Q. N-Isopropylacrylamide-modified polyethylenimine-mediated p53 gene delivery to prevent the proliferation of cancer cells. Colloids Surf B Biointerfaces 2015; 129: 54-62.
[33] Levine B and Yuan J. Autophagy in cell death: an innocent convict? J Clin Invest 2005; 115: 2679-2688.
[34] Zorko M and Langel U. Cell-penetrating peptides: mechanism and kinetics of cargo delivery. Adv Drug Deliv Rev 2005; 57: 529-545.